Optics & Laser Technology 92 (2017) 163–167

Contents lists available at ScienceDirect

Optics & Laser Technology

journal homepage: www.elsevier.com/locate/optlastec

Full length article

Femtosecond-laser-written superficial cladding waveguides in Nd:CaF_2 crystal

Rang Li[a], Weijie Nie[a], Qingming Lu[b], Chen Cheng[a], Zhen Shang[a], Javier R. Vázquez de Aldana[b,c], Feng Chen[a,c,*]

[a] School of Physics, State Key Laboratory of Crystal Materials, Shandong University, Jinan 250100, China
[b] School of Chemistry and Chemical Engineering, Shandong University, Jinan 250100, China
[c] Laser Microprocessing Group, Departamento de Física Aplicada, Universidad de Salamanca, Salamanca 37008, Spain

ARTICLE INFO

Keywords:
Optical waveguides
Nd:CaF_2 crystal
Femtosecond laser writing

ABSTRACT

We report on the superficial cladding waveguides fabricated by direct femtosecond laser writing in Nd: CaF_2 crystal with three different groups of parameters. The lowest propagation loss of waveguides has been determined to be 0.7 dB/cm at wavelength of 632.8 nm along TE polarization. The near fundamental modal distributions have been imaged through the end-face coupling technique. The guidance of the waveguides is found to possess low sensitivity on polarization of the probe light. By using a confocal microscope system, the micro-photoluminescence mappings and micro-fluorescence spectra are also obtained, which indicates the photoluminescence features of the Nd^{3+} ions are well preserved in the waveguide cores after direct femtosecond laser writing.

1. Introduction

As the basic components in integrated photonics [1,2], the waveguide structures offer platforms for confining the light propagation in small volumes [3]. Benefiting from the high intracavity optical intensities and diffraction-free beam propagation, waveguides have been applied in a number of optical systems to realize various applications, including signal processing, bean splitters, and ring resonators [4–6]. Several techniques, for example, ion implantation [7], metal-ion indiffusion [8], epitaxial layer deposition [9] and femtosecond laser writing [10–12], have been utilized to construct diverse optical waveguide structures in various materials. Particularly, compared with the one-dimensional waveguide structures (planar or slab) [13], the two-dimensional waveguide structures (channel or ridge) show compact spatial confinement of light, which attracts more attention among researchers [3].

Since the pioneering work by Davis et al. [14], femtosecond laser writing has emerged to be one of the most attractive methods to fabricate the cladding waveguide structure in glass due to its advantage of the direct, rapid and mask-free features [15]. Either positive or negative refractive index change can be created in glass through modifying the lattice distortion, stress effects and volume expansion by femtosecond laser writing. Numerous works of fabrication of depressed cladding waveguides and waveguides with positive refractive index change in glass have been performed in the past few years [16–18]. More importantly, femtosecond laser writing has shown similar excellent ability of refractive index changing in crystal materials so that the crystalline waveguides have received considerable attention until now [3]. According to the work by Okhrimchuk et al. [19], the core of the cladding waveguide is surrounded by a great quantity of femtosecond laser written tracks with low refractive index, which is different from the waveguide with positive refractive index changes in the track [20] and the waveguide of dual-line structure [21]. It is promising to form the fiber-waveguide-fiber structure in integrated photonic systems when combined with fibers [22]. Furthermore, for many optoelectronic applications, such as large area mode amplifiers, lasers, sensors and electro-optic modulators, the waveguides or photonic circuits are required to be near the surface of the host material. In consequence, the superficial cladding waveguides, with the excellent wave-guiding characteristics, are fabricated by femtosecond laser writing, which indicates the potential applications of the superficial cladding structures [23].

In recent years, the lanthanide-doped calcium fluoride crystals have gained recognition on the account of the superior optical properties [24,25]. First, CaF_2 crystals present a wide optical transparency range from 125 nm to 9000 nm and the transmittance hardly changed with the wavelength increasing [26]. Second, with relatively low refractive index, the dispersion has an insensitive variation with the wavelength

* Corresponding author at: School of Physics, State Key Laboratory of Crystal Materials, Shandong University, Jinan 250100, China.
E-mail address: drfchen@sdu.edu.cn (F. Chen).

http://dx.doi.org/10.1016/j.optlastec.2017.01.026
Received 16 August 2016; Received in revised form 28 November 2016; Accepted 24 January 2017
Available online 01 February 2017
0030-3992/ © 2017 Elsevier Ltd. All rights reserved.

and the temperature changing. Last but not the least, the low phonon energy of CaF_2 minimizes multi-phonon de-excitation probabilities and the energy transfer rate increases when doped with lanthanide ions because of the charge compensation effects. In addition, the non-hygroscopic, resistance to chemical attack and other chemical properties make it a stable material in multi-application [27]. However, as one of the promising scintillation host material, CaF_2 crystal has long decay time due to self trapped excition emission with a peak of 270 nm. Nd^{3+} ions could activate wide band gap materials emitting in the vacuum ultraviolet region to improve the material luminescence properties and shift the emission spectrum.

In our work, we report on the fabrication of the superficial cladding waveguides in Nd:CaF_2 crystal by direct femtosecond laser writing, which presents the significant regularity with diverse parameters. Besides, at an common 632.8 nm wavelength that no absorption are observed, the near fundamental modal distributions, the low sensitivity on polarization of the probe light and the well-preserved photoluminescence features in the waveguide cores with respect to the bulk are studied in detail as well.

2. Experiments in details

The CaF_2 crystal used in this work was doped by 1 at% Nd^{3+} ions and cut into wafers with dimensions of 10×10×2 mm^3. Before being optically polished, the superficial cladding waveguide structures were fabricated by the amplified Ti:sapphire laser system of the Universidad de Salamanca, Spain. As Fig. 1(a) depicts, during the writing process, the linearly-polarized 120-fs pulses were generated at a central wavelength of 800 nm with the repetition rate of 1 kHz. In order to get a fine control of the incident energy, a calibrated neutral density filter was set after a half-wave plate and a linear polarizer so that the maximum available pulse energy of 1 mJ could reduce to an ideal value. The sample was placed in a computer controlled motorized 3-axes stage, whilst the laser beam was focused with a 40× microscope objective. The scanning velocity was adjusted to a constant of 500 μm/s, and the desired circular geometry was achieved with a lateral separation of 3 μm between each two adjacent damage tracks at the same time. To investigate the influence of the pulse energy of the femtosecond writing, and the depth and the diameter of the waveguide, we fabricated eight waveguides with comparable parameters, which is shown in Table 1.

With the purpose of characterizing the superficial cladding waveguides, we used an optical microscope (Axio Imager, Carl Zeiss) to photograph the structures. Furthermore, the end-face coupling arrangement was employed to investigate the near-field modal profiles of the superficial cladding waveguides under 632.8-nm wavelength along TE and TM polarization respectively. As shown in Fig. 1(b), the launched light from He-Ne laser was coupled into the waveguide structure, in the meanwhile the half-wave plate, which was put between the 632.8-nm laser and lens, was rotated to convert the polarization of the input light. In this way, the all-angle guidance were investigated and the modes were imaged by CCD (CinCam CMOS, Cinogy), while the propagation losses were calculated by measuring the output power and input power. The CCD and power meters (4π, LaserPoint) were placed after the objective 2 respectively.

Table 1
Fabrication parameters of the Nd:CaF_2 waveguides by femtosecond laser writing.

Pulse energy of 0.21 μJ			Pulse energy of 0.17 μJ		
Waveguide	Depth (μm)	Diameter (μm)	Waveguide	Depth (μm)	Diameter (μm)
No.1	7.5	30	No.5	7.5	30
No.2	7.5	50	No.6	7.5	50
No.3	3.0	30	No.7	3.0	30
No.4	3.0	50	No.8	3.0	50

In order to study the physical mechanism of femtosecond laser inscription in Nd:CaF_2 crystal, we used the confocal microscope system at 500-nm wavelength to estimate the fluorescence properties. For comparison, the spectra of the bulk and the track regions were measured as well.

3. Results and discussion

Fig. 2(a)–(h) depict the optical microscope images of the cross sections of the Nd:CaF_2 superficial cladding structures. The numbers of the damage tracks are 19 and 27 for waveguides with smaller diameter and larger diameter respectively. These tracks are covering an angle of ~75° with an error of ± 5°. The detailed parameters of the waveguides are displayed in Table 1. Hence eight microscope images of the superficial cladding waveguides with different energy, diameter and depth are presented here.

Fig. 2(i) depicts the relevance of output power and polarization. For concise illustration, we only display the variation curve of No. 8 waveguide, for all eight waveguide structures perform a similar changing tendency. As the Fig. 2(i) shows, it is clearly that the polarization-dependent effect of transmission is not obvious. Based on the nearly constant input power ~1.88 mW, the output power, along TE polarization (0°), is slightly higher than that along TM polarization (90°), which may be due to several reasons such as the noncentrosymmetrical structure of the waveguide. The output power curve varies smoothly as we convert the polarization from TE to TM by rotating the half-wave plate. For example, the output power decreases from 1.13 mW (TE) to 1.04 mW (30°) and reduces continuously to 0.98 mW (60°), and the lowest output power is 0.92 mW (TM). Considering the coupling efficiency and experimental error, we may conclude that the Nd:CaF_2 superficial cladding waveguides by femtosecond writing have the good feature of low sensitivity on polarization of the probe light.

Fig. 3(a)–(p) depict the measured modal distributions of the circular superficial cladding waveguides under 632.8-nm wavelength along TM and TE polarizations, respectively. As one can see, the waveguiding characteristics of the Nd:CaF_2 superficial cladding waveguides are similar at both two conditions which is different from the other waveguides, i.e., the dual-line waveguides, as they only support

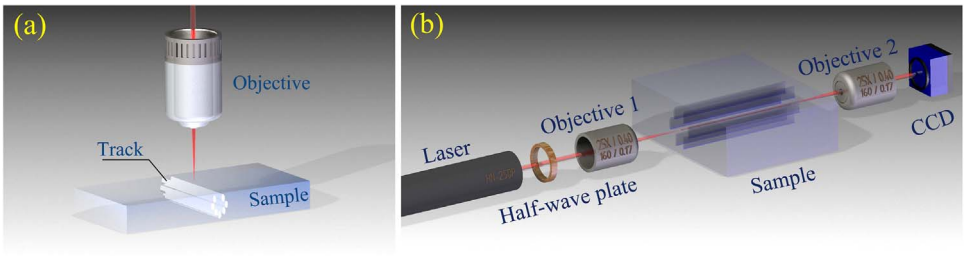

Fig. 1. (a) The schematic plot of a femtosecond laser-writing superficial cladding waveguide in Nd:CaF_2 crystal; (b) the end face coupling arrangement used to investigate the guiding properties.

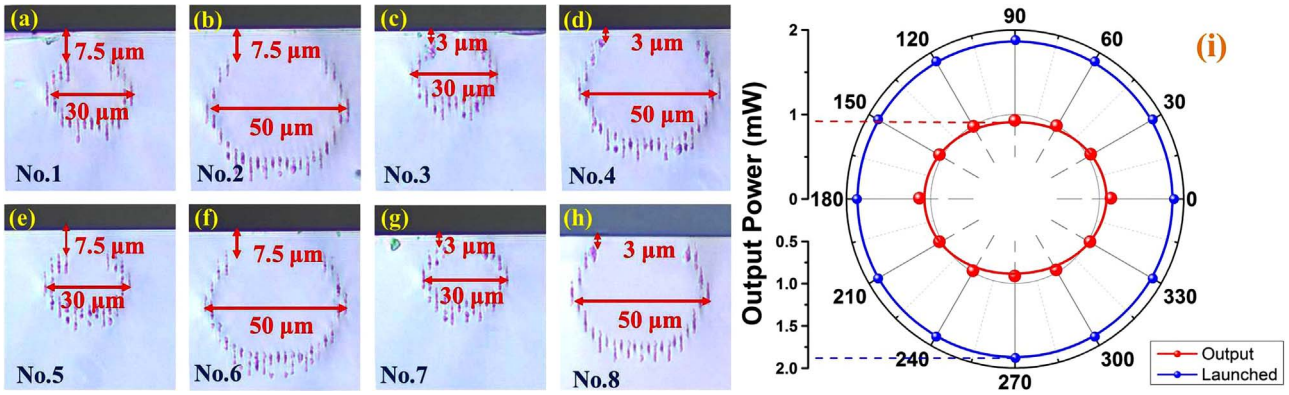

Fig. 2. The microscopic images (a)-(h) of the No.1 to No. 8 superficial cladding waveguides at the cross sections; (i) the output power as a function of all-angel light transmission with the same launched power of superficial cladding waveguide No. 8 at 632.8 nm.

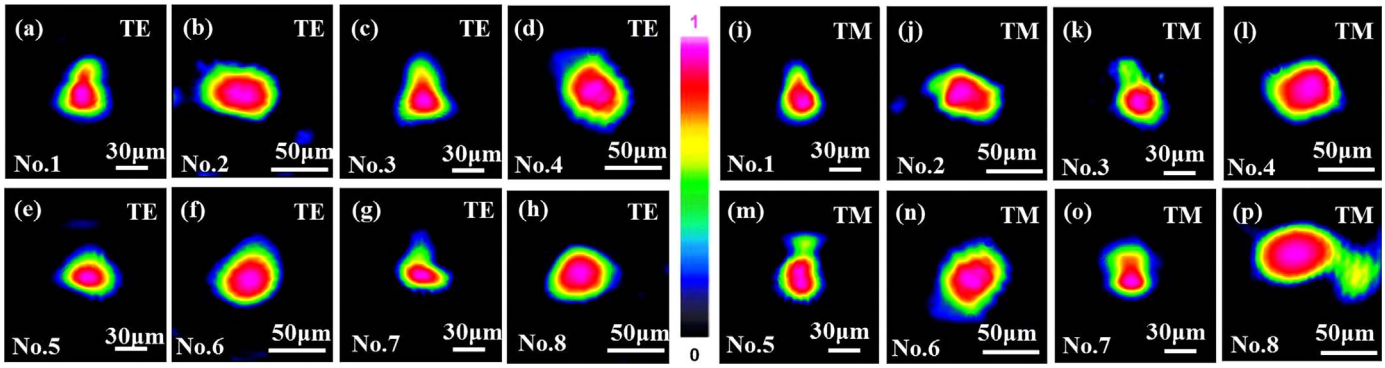

Fig. 3. Measured near-field intensity distributions of superficial cladding waveguides Nos. 1–8 at 632.8 nm. (a)-(h) are along TE polarization and (i)-(p) are along TM polarization.

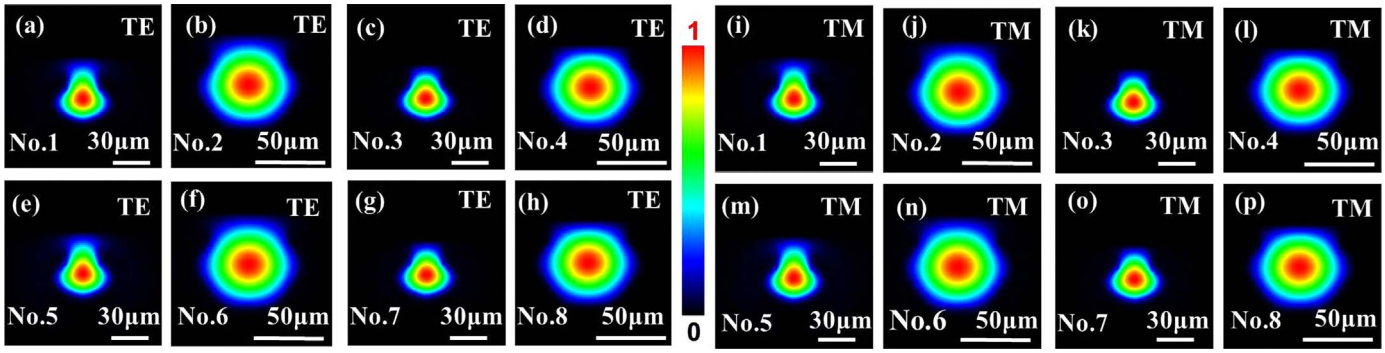

Fig. 4. Simulated near-field intensity distributions of superficial cladding waveguides Nos. 1–8 at 632.8 nm. (a)-(h) are along TE polarization and (i)-(p) are along TM polarization.

Table 2
The propagation loss α (dB/cm) of the Nd: CaF_2 superficial cladding waveguides by femtosecond laser writing at TE and TM polarization respectively.

	No. 1	No. 2	No. 3	No. 4	No. 5	No. 6	No. 7	No. 8
TE	3.2	2.6	2.8	1.6	3.4	2.8	3.1	1.9
TM	2.0	1.6	1.8	0.7	2.2	1.9	2.0	0.9

guidance parallel to the damage tracks or much weak for one polarization [28,29]. However, with a smaller diameter, the modal distribution matches near fundamental mode, compared with the waveguide which owns a larger diameter. Although No.8 waveguide seems to have a trend to show multimode, the relatively zygomorphic single modes of the most waveguides indicated that the main energy of the light fields is well confined in the fundamental modes, which coincides with our previous work with the similar scales [22]. It is reasonable that some of the waveguides seem to have light leaking from the upper region because of the lack of the tracks at this region. The results are compared with the simulation calculated by Rsoft© software based on the finite-difference beam propagation method (FD-BPM). The maximum refractive index contrast could be roughly approximated by using the equation $\Delta n \approx \sin^2\theta_m/2n$, where θ_m is the maximum incident angular deflection and n is the refractive index of the substrate (1.4329). The refractive index contrasts at the wavelength of 632.8 nm were about 5×10^{-3} and 7×10^{-3} for waveguides Nos. 1–4 and Nos. 5–8 respectively. As Fig. 4(a)–(p) show, the measured near-field intensity distributions have reasonable agreement with the distributions simulated along both TE and TM polarization.

To determine the propagation loss of the superficial cladding waveguide, we measured the powers of the in-coupled and output light. The propagation loss can be calculated by using the formula

$$\alpha = -\frac{10}{L}\log_{10}\left[\frac{P_{out}}{P_{in}\cdot(1-R)^2\cdot\eta}\right] \quad (1)$$

where P_{in} is the in-coupled light power and P_{out} is the output light power. The length of light propagating in the sample is written as L. R

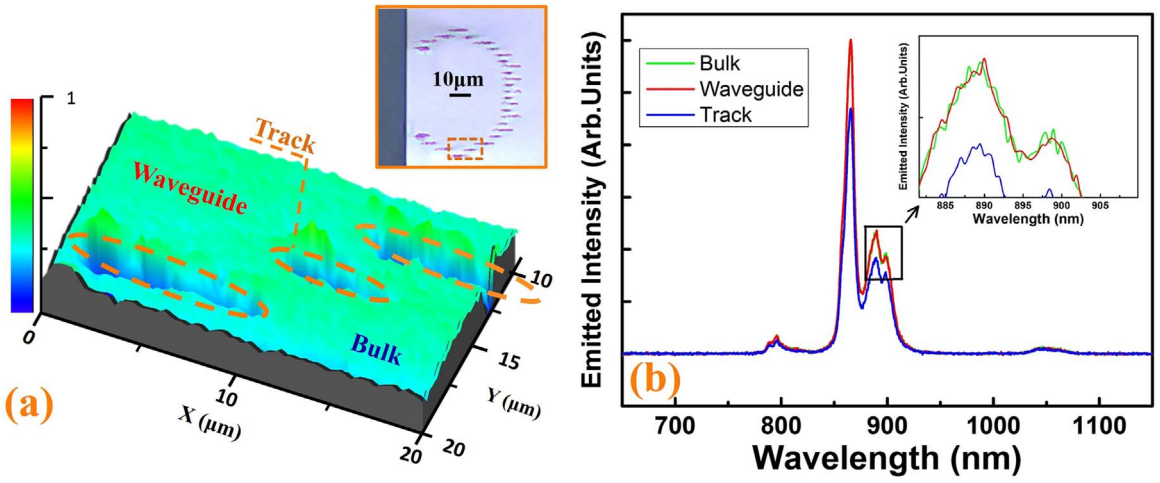

Fig. 5. (a) Micro-photoluminescence mapping (the spatial distributions of intensity corresponding to $^4F_{3/2}\rightarrow{}^4I_{9/2}$); (b) the confocal micro-luminescence spectra of Nd: CaF_2 crystal at room temperature in the No. 8 waveguide region, track region and bulk region.

is the reflectance (~0.031664 at 632.8 nm) and η is the coupling efficiency which can be approximately calculated by the equation $\eta = [2\omega_1\cdot\omega_2/(\omega_1 + \omega_2)]^2$. ω_1, ω_2 are the modal diameter of the in-coupled light and output light respectively. The result is exhibited in Table 2.

It is apparently that the propagation loss is lower with higher energy when the other conditions are the same. It is supposed that the phenomenon is caused by the weaker extent of damage to the lattice structure with a lower energy so that the refractive index decreases less. That is to say, with higher energy, the refractive index of the track is smaller than the one with lower energy, which indicates the prior light confinement effect. As for diameter, the propagation loss decreases with the increase of the diameter from 30 μm to 50 μm, with the same depth and energy. The reason, we believe, is that the smaller waveguide possess a smaller acceptance angle and some high order modes are cut off leaving the near fundamental modes, which coincides with the modal profiles we mentioned before. Moreover, the deeper one shows a lower loss. The superior light confinement is result in the greater difference between the waveguide core and its surrounding region, and the light confinement of the deeper one is less influenced by the air. Therefore the deeper waveguide possesses a prior propagation property due to the lower refractive index of the air compared with the one of the substrate. In addition, along with the diameter changing, the decrease ratio of the propagation loss is larger with the smaller depth. With the same depth, the decrease ratio is approximate and the energy seems to have unobvious effect to the ratio. In addition, the above conclusion is valuable for both TE and TM polarization, although the propagation loss is relatively lower along TE polarization (see Table 2).

Fig. 5(a)–(b) demonstrates the micro-photoluminescence mappings and the emission luminescence spectra of the Nd^{3+} ions related to $^4F_{3/2}\rightarrow{}^4I_{9/2}$ band as obtained from the core of the waveguide, bulk and track. It can be seen that the area induced by femtosecond-laser have an obvious modification of PL emission and the full picture is inserted in Fig. 5(a). On account of the overlap of the waveguides No. 1 to No. 8 curves, we just display the spectra of No. 8 for its relative superior properties mentioned above. As shown in Fig. 5(b), the emitted intensity of the track is the lowest whilst the intensity of the waveguide is a little higher than the bulk. We surmise that it is caused by improvement of the optical coupling efficiency due to the stress effect by femtosecond laser writing and the confinement of fluorescence within the structures [30,31]. However, the difference of the luminescence spectra is unobvious, which indicates the femtosecond laser writing technology has not caused microstructural changes in Nd:CaF_2 crystal and the performance of the photoluminescence has been well preserved.

4. Conclusion

In summary, we report on the fabrication of the superficial cladding waveguides in Nd:CaF_2 crystal by femtosecond laser writing. The guiding properties are investigated by end-face coupling arrangement which shows near fundamental modal distributions along both TE and TM polarizations. The lowest propagation losses are measured to be 0.7 dB/cm, with three different parameters (energy, diameter and depth) considered. In addition, the low sensitivity on polarization and the well-preserved photoluminescence performance indicate the potential application in integrated photonic systems.

Acknowledgements

The work is supported by Specialized Research Fund for the Doctoral Program of Higher Education of China (20130131130001); the 111 Project (No. B13029); Fundamental Research Funds for Shandong University (No. 2014JC002). JRVA thanks support from Junta de Castilla y León (Project SA116U13).

References

[1] E.J. Murphy, Integrated Optical Circuits and Components: dDesign and Applications, Marcel Dekker, New York, 1999.
[2] G. Lifante, Integrated Photonics: Fundamentals (Atrium), John Wiley & Sons Ltd, England, 2003.
[3] F. Chen, J.R. Vázquez, de Aldana, Laser Photonics Rev. 8 (2014) 251–275.
[4] J.L. Liu, J.M. Dai, S.L. Chin, X.C. Zhang, Nat. Photonics 4 (2010) 627–631.
[5] R. Singh, R.A. Yadav, D.P. Singh, J. Russ., Laser Res. 34 (2013) 509–514.
[6] D. Popa, Z. Sun, T. Hasan, F. Torrisi, F. Wang, A.C. Ferrari, Appl. Phys. Lett. 98 (2011) 073106.
[7] G.B. Montanari, P. De Nicola, S. Sugliani, A. Menin, A. Nubile, G. Bellanca, M. Bianconi, G.G. Bentini, Opt. Express 20 (2012) 4444–4453.
[8] D. Zhang, C. Wong, E.Y. Pun, Mater. Res. Bull. 60 (2014) 771–777.
[9] H. Akazawa, H. Fukuda, Aip. Adv. 5 (2015) 057163.
[10] J. Siebenmorgen, T. Calmano, K. Petermann, G. Huber, Opt. Express 18 (2010) 16035–16041.
[11] A. Szameit, S. Nolte, J. Phys. B-At. Mol. Opt. 43 (2010) 163001.
[12] K. Sugioka, Y. Cheng, Light Sci. Appl. 3 (2014) e419.
[13] J.M. Hallas, K.A. Baker, J.H. Karp, E.J. Tremblay, J.E. Ford, Appl. Opt. 51 (2012) 6117–6124.
[14] K.M. Davis, K. Miura, N. Sugimoto, K. Hirao, Opt. Lett. 21 (1996) 1729–1731.
[15] G. Salamu, F. Jipa, M. Zamfirescu, N. Pavel, Opt. Mater. Express 4 (2014) 790–797.
[16] R. Osellame, G. Cerullo, R. Ramponi, Femtosecond-laser Micromachining: Photonic and Microfluidic Devices in Transparent Materials, Springer, Berlin, 2012.
[17] D.G. Lancaster, S. Gross, H. Ebendorff-Heidepriem, K. Kuan, T.M. Monro, M. Ams, A. Fuerbach, M.J. Withford, Opt. Lett. 36 (2011) 1587–1589.
[18] M. Bukharin, D. Khudakov, S. Vartapetov, Phys. Procedia 71 (2015) 272–276.
[19] A.G. Okhrimchuk, A.V. Shestakov, I. Khrushchev, J. Mitchell, Opt. Lett. 30 (2005) 2248–2250.

[20] J.R. Macdonald, R.R. Thomson, S.J. Beecher, N.D. Psaila, H.T. Bookey, A.K. Kar, Opt. Lett. 35 (2010) 4036–4038.
[21] G. Salamu, F. Jipa, M. Zamfirescu, N. Pavel, Opt. Express 22 (2014) 5177–5182.
[22] H.L. Liu, Y.C. Jia, J.R. Vázquez de Aldana, D. Jaque, F. Chen, Opt. Express 20 (2012) 18620–18629.
[23] C. Cheng, C. Romero, J.R. Vázquez de Aldana, F. Chen, Opt. Eng. 54 (2015) 067113.
[24] L.E. Bausa, R. Legros, A. Munoz-Yague, Appl. Phys. Lett. 70 (1991) 4485–4489.
[25] Q.G. Wang, L.B. Su, H.J. Li, L.H. Zheng, X. Guo, D.P. Jiang, H.Y. Zhao, J. Xu, W. Ryba-Romanowski, P. Solarz, R. Lisiecki, J. Alloy. Compd. 509 (2011) 8880–8884.
[26] P. Samuel, H. Ishizawa, Y. Ezura, K.I. Ueda, S.M. Babu, Opt. Mater. 33 (2011) 735–737.
[27] N.N. Dong, M. Pedroni, F. Piccinelli, G. Conti, A. Sbarbati, J.E. Ramirez-Hernandez, L.M. Maestro, M.C. Iglesias-dela Cruz, F. Sanz-Rodriguez, A. Juarranz, F. Chen, F. Vetrone, J.A. Capobianco, J.G. Sole, M. Bettinelli, D. Jaque, A. Speghini, ACS Nano 5 (2011) 8665–8671.
[28] J. Thomas, M. Heinrich, P. Zeil, V. Hilbert, K. Rademaker, R. Riedel, S. Ringleb, C. Dubs, J. Ruske, S. Nolte, A. Tuennermann, Phys. Status Solidi A. 208 (2011) 276–283.
[29] J. Burghoff, S. Nolte, A. Tuennermann, Appl. Phys. A-Mater. 89 (2007) 127–132.
[30] D. Jaque, F. Chen, Y. Tan, Appl. Phys. Lett. 92 (2008) 161908.
[31] B. Sotillo, V. Bharadwaj, J.P. Hadden, M. Sakakura, A. Chiappini, T.T. Fernandez, S. Longhi, O. Jedrkiewicz, Y. Shimotsuma, L. Criante, R. Osellame, G. Galzerano, M. Ferrari, K. Miura, R. Ramponi, P.E. Barclay, S.M. Eaton, Sci. Rep. 6 (2016) 35566.